Non-radiative relaxation processes in luminescence of InP/ZnS quantum dots

Non-radiative relaxation processes in luminescence of InP/ZnS quantum dots

S S Savchenko[1], A S Vokhmintsev[1] and I A Weinstein[1,2]

[1]NANOTECH Centre, Ural Federal University, 19 Mira str., Ekaterinburg 620002, Russia
[2]Institute of Metallurgy of the Ural Branch of the Russian Academy of Sciences, 101 Amundsen str., Ekaterinburg 620016, Russia

E-mail: s.s.savchenko@urfu.ru

Abstract. Photoluminescence (PL) thermal quenching of InP/ZnS core/shell nanocrystals of 4.2 (QD-1) and 4.6 (QD-2) nm in diameter is investigated in the temperature range of 6.5–296 K. Observed PL spectra are found to originate from exciton and defect-related transitions. Temperature behavior of the emission bands indicates effects of inhomogeneous broadening due to distributions of quantum dots parameters in the ensembles. PL thermal quenching analysis unveils two non-radiative relaxation channels for each band in both samples. Activation energies of 130 and 119 meV in QD-1 and QD-2, correspondingly, for the exciton band can be assigned to the bright-bright splitting of the exciton fine structure.

Colloidal indium phosphide-based nanocrystals are environmentally friendly material with tunable optical properties due to a quantum confinement effect. Potential applications of these quantum dots (QDs) in various fields of optoelectronics, photonics, theranostics, et al. can be enhanced by further improving their structure [1–4]. Active work is being done in a refining their synthesis protocols to increase emission quantum yield. In this regard, study of photoluminescence (PL) thermal quenching is of fundamental interest since it probes characteristics of states responsible for activation of non-radiative energy loss pathways.

Photoluminescence was studied for two ensembles of InP/ZnS core/shell QDs with average particle diameters of 4.2 (QD-1) and 4.6 (QD-2) nm estimated from the position of the first exciton absorption band [5]. Samples were prepared by drop casting the solution on quartz plates. Emission spectra were analyzed using a Shamrock SR-303i-B spectrograph equipped with a cooled Newton^{EM} DU-970P-BV-602 CCD camera by Andor. Measurements were carried out at temperatures in a range from 6.5 to 296 K controlled by means of a Janis CCS-100/204N closed cycle refrigerator system. The samples were excited by a light-emitting diode of 372 nm intensity maximum and 5 mW/cm^2 average power density. Luminescence quantum yield of the nanocrystals was measured with respect to the standard according to the known procedure [6]. Rhodamine 6G was used as a reference [7].

Temperature evolution of PL curves for QD-1 and QD-2 films is displayed in figure 1. At room temperature the emission spectra have an asymmetric shape characterized by a less steep low-energy part. Luminescence intensity maximum for QD-1 is observed at E_x = 2.32 eV, spectrum half-width H = 296 meV. The larger QD-2 nanocrystals exhibit E_x = 2.13 eV and H = 364 meV. Upon cooling E_x moves to 2.36 eV for the QD-1 and to 2.16 eV for the QD-2 at 6.5 K. Herewith, spectra shape distinctly reveals tails at temperatures below 160 and 100 K for the samples, respectively. They are

redshifted by about 300 meV from PL maxima. In QD-1 this shoulder turns into a band with a local maximum at E_d = 2.07 eV for 6.5 K. A position of this emission band in the QD-2 is determined by means of the second derivative calculation as E_d = 1.8 eV [8]. Due to such changes, half-widths of the QD-1 and QD-2 spectra are increased up to 705 and 559 meV. Figure 2 insets represent the spectra normalized to their maximum values. The plots highlight the difference between low-energy parts of the spectra in the ensembles under study. One can see that the E_d is more pronounced in the QD-1 sample with smaller nanocrystals. The intensity increases monotonically with decreasing temperature from 296 K to 6.5 K.

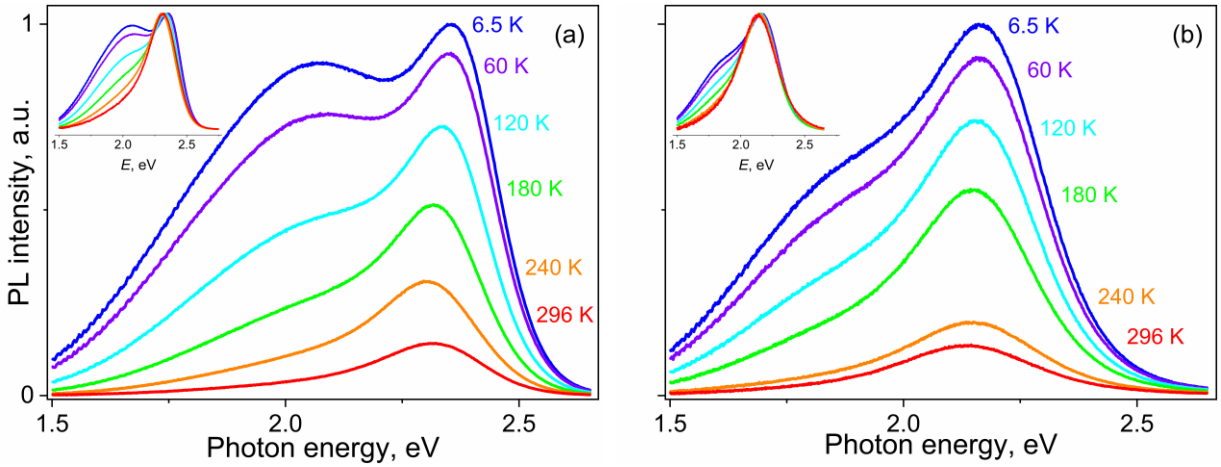

Figure 1. PL spectra of QD-1 (a) and QD-2 (b) InP/ZnS ensembles at different temperatures. Insets clearly shows change of spectra in the low-energy part.

The PL spectra can be well reproduced using several Gaussian components. However, they cannot give physically rational explanation of the temperature evolution in frame of exciton-phonon interaction [9, 10]. Such a situation may result from inhomogeneous broadening, which is manifested in ensemble optical spectra of InP/ZnS nanocrystals [5, 11–13]. According to the reported findings, the high-energy band E_x can be attributed to exciton emission, and the low-energy band E_d is probably related to defects in the crystal lattice of the InP core [9, 10, 14, 15].

Efficiency of radiative recombination processes for the studied ensembles strongly depends on temperature, which is expressed in the change of their luminescence intensity upon cooling. The significant influence of non-radiative relaxation channels is evidenced by PL quantum yield amounted to 27% for QD-1 and 10% for QD-2 at room temperature. In order to study quenching of the QDs luminescence, temperature dependences for the following values are analyzed: the I_{int} integrated intensity, which characterizes the area under the PL spectrum; the I_x intensity at the maximum related to the exciton band E_x, and the I_d intensity of the E_d band associated with the emission involving defect states. The corresponding temperature data normalized at 6.5 K values are presented in figure 2. The insets show these dependencies in Arrhenius coordinates. Our samples distinctly reveal complex thermal quenching behavior implying at least two non-radiative relaxation pathways of energy loss for both QD-1 and QD-2.

In the temperature range under consideration, the exciton and defect-related luminescence intensities in both ensembles increase with decreasing temperature by about 7 and 18 times, respectively. Simultaneously, the integrated intensity increases by 13 times for QD-1 and by 9 for QD-2. Such a situation strengthens the idea of inhomogeneous broadening indicating multicomponent structure of the emission. Therefore, considering band centers we access a certain subset of nanocrystals in the ensemble, which are equal in terms of energy structure. To determine activation energies of non-radiative relaxation channels the obtained data were fitted with Mott expression [10]:

$$I(T) = I_0\left[1 + \sum_i p_i \exp\left(-\frac{E_{qi}}{kT}\right)\right]^{-1} \quad (1)$$

where I_0 is the intensity at 0 K; p_i is preexponential factor for the ith non-radiative relaxation channel; k is the Boltzmann constant, eV/K; E_{qi} is the activation energy for the ith channel, eV. The studied dependences are described with good accuracy (Adj. R-square> 0.996) according to (1) under the assumption of two channels (see solid lines in figure 2). The approximation parameters are summarized in table 1.

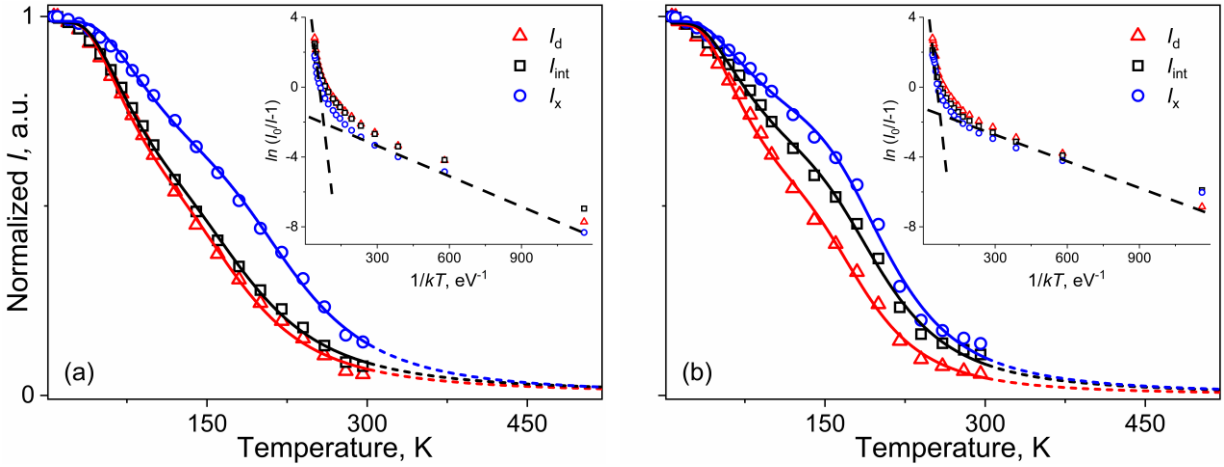

Figure 2. PL thermal quenching of QD-1 (a) and QD-2 (b). Symbols are experimental data, solid lines correspond to fits with equation (1). Insets show the dependencies in Arrhenius coordinates.

Table 1. Activation energy of non-radiative relaxation channels in InP/ZnS QDs.

	Intensity	E_{q1}, meV	E_{q2}, meV
QD-1	I_d, I_{int}	16 ± 1	95 ± 21
	I_x	19 ± 2	130 ± 27
QD-2	I_d, I_{int}	15 ± 2	113 ± 17
	I_x	13 ± 2	119 ± 11

The activation energies are found to have the same magnitudes for I_d and I_{int}. This fact supports the dominating contribution of defect-related band in PL quenching of the InP/ZnS ensembles. The obtained E_{q1} values for I_x and I_d characterize non-radiative relaxation of excitations via the corresponding energy barriers, which can be assigned to surface and/or defect states [16]. Earlier, we have experimentally analyzed the temperature dependence of the optical absorption spectra and extracted effective phonon energies of 15 and 59 meV responsible for temperature-induced shift of the exciton levels in QD-1 and QD-2, respectively [9, 12]. These vibration modes bear enough energy to activate relaxation processes under discussion.

A noteworthy observation is that E_{q2} values for exciton PL quenching are dependent on size and decrease with increasing average diameter of the studied QDs. Moreover, the values are consistent with the energy separation Δ_{bb} between upper bright exciton state and dark-bright doublet unveiled by studying the exciton fine structure in InP/ZnS nanocrystals [15]. According to the size effect, the Δ_{bb} splitting increases when InP core decreases. The samples [15] that are close to the QD-1 and QD-2 ensembles in terms of exciton PL band position feature Δ_{bb} = 147 and 85 meV, correspondingly.

Dash lines in figure 2 illustrate extrapolation of the fitted quenching curves for higher temperatures. They predict about 3-fold intensity drop of QDs luminescence when heated up to 400 K. Thus, to refine the obtained values of activation energies high-temperature study of non-radiative relaxation processes is needed. In addition, considering the observed features of the temperature

evolution of the luminescence spectrum and the size distribution of QDs, one should also expect the distribution of activation energies for the corresponding PL quenching mechanisms in InP/ZnS nanocrystal ensembles.

In conclusion, the photoluminescence quenching of InP/ZnS nanocrystals films with average particle diameters in ensembles of 4.2 (QD-1) and 4.6 (QD-2) nm and PL quantum yields of 27 and 10% at room temperature, respectively, are studied. The spectra evolution in the temperature range from 296 to 6.5 K allows us to conclude that the luminescence is formed by two bands E_x and E_d attributed to radiative recombination from exciton and defect states. The bands intensity drops 7 and 18 times upon heating in the studied range, meanwhile integrated intensity decreases 13 times for QD-1 and 9 times for QD-2. Quenching processes analysis reveals two non-radiative relaxation channels for each transition type in both ensembles. Low-energy barriers can be ascribed to surface and/or defect states. Non-radiative relaxation competing the E_x emission may involve intrinsic upper bright state of the exciton fine structure.

Acknowledgments
This research was supported by RFBR according to the research project № 18-32-00664 and Act 211 Government of the Russian Federation, contract no. 02.A03.21.0006. I.W. thanks the Minobrnauki initiative research project for support.

References
[1] Alivisatos A P 1996 *Science* **271** 933–7
[2] Michalet X, Pinaud F F, Bentolila L A, Tsay J M, Doose S, Li J J, Sundaresan G, Wu A M, Gambhir S S and Weiss S 2005 *Science* **307** 538–44
[3] Scher J A, Bayne M G, Srihari A, Nangia S and Chakraborty A 2018 *J. Chem. Phys.* **149** 014103
[4] Hughes K E, Stein J L, Friedfeld M R, Cossairt B M, Gamelin D R 2019 *ACS Nano* **13** 14198–207
[5] Savchenko S S and Weinstein I A 2019 *Nanomaterials* **9** 716
[6] Grabolle M, Spieles M, Lesnyak V, Gaponik N, Eychmüller A and Resch-Genger U 2009 *Anal. Chem.* **81** 6285–94
[7] Brouwer A M 2011 *Pure. Appl. Chem.* **83** 2213–28
[8] Savchenko S S, Vokhmintsev A S and Weinstein I A 2017 *Tech. Phys. Lett.* **43** 297–300
[9] Savchenko S S, Vokhmintsev A S and Weinstein I A 2018 *J. Phys. Conf. Ser.* **961** 012003
[10] Savchenko S S, Vokhmintsev A S and Weinstein I A 2018 *AIP Conf. Proc.* **2015** 020085
[11] Brichkin S B, Spirin M G, Tovstun S A, Gak V Y, Mart'yanova E G and Razumov V F 2016 *High Energy Chem.* **50** 395–9
[12] Savchenko S S, Vokhmintsev A S and Weinstein I A 2017 *Opt. Mater. Express* **7** 354–9
[13] Savchenko S S, Vokhmintsev A S and Weinstein I A 2018 *Optics InfoBase Conference Papers* **Part F107-NOMA 2018** NoW1J.4
[14] Pham T T, Chi Tran T K and Nguyen Q L 2011 *Adv. Nat. Sci. Nanosci. Nanotechnol.* **2** 025001
[15] Biadala L, Siebers B, Beyasit Y, Tessier M D, Dupont D, Hens Z, Yakovlev D R and Bayer M 2016 *ACS Nano* **10** 3356–64
[16] Valerini D, Cretí A, Lomascolo M, Manna L, Cingolani R and Anni M 2005 *Phys. Rev.* B *Condens. Matter Mater. Phys.* **71** 235409